

ARTICLE

Ion-Pair Photodissociation of Trichloromonofluoromethane

Liu-li Chen^a, Shan-xi Tian^{a*}, Yun-feng Xu^a, Gen-bai Chu^b, Fu-yi Liu^b, Xiao-bin Shan^b,
Liu-si Sheng^b

a. Hefei National Laboratory for Physical Sciences at the Microscale and Department of Chemical Physics, University of Science and Technology of China, Hefei 230026, China

b. National Synchrotron Radiation Laboratory, University of Science and Technology of China, Hefei 230029, China

(Dated: Received on March 17, 2011; Accepted on April 6, 2011)

Anionic fragments, F⁻ and Cl⁻ including two isotope species ³⁵Cl⁻ and ³⁷Cl⁻, are observed in the photoexcitations of CFC₃. The ion-pair anion efficiency spectra of ³⁵Cl⁻ and ³⁷Cl⁻ are recorded in the photon energy range of 7.75–22.00 eV. The threshold of ion-pair dissociation CFC₃→CFCl₂⁺+Cl⁻ is experimentally determined to be 7.94±0.04 eV. With the references of the high-resolution photoabsorption spectra reported in the literatures, we make tentative assignments of the electron valence-to-Rydberg transitions. Furthermore, the multibody ion-pair fragmentation processes to Cl⁻ are discussed by comparison between the calculated thermochemical thresholds and the experimental efficiency spectrum.

Key words: Trichloromonofluoromethane, Ion-pair dissociation, Rydberg state, Ion-pair anion efficiency spectrum, Time-of-flight mass spectrometer

I. INTRODUCTION

Trichloromonofluoromethane CFC₃, known as Freon 11, is of particular interest because it together with the other single carbon Freons plays role in the catalytic decomposition of atmospheric ozone in the stratosphere [1]. Photochemistry and the related dynamics of CFC₃ have been extensively investigated. Photoelectron spectra were recorded using the discharge ultraviolet (UV) Helium lamps, providing basic information of the electron promotions from the valence molecular orbitals (MOs) [2–5]. General information on electron excitations from the photoabsorption spectrum of CFC₃ [2, 6–8] can be further inspected and classified with the different experimental techniques such as fluorescence excitation spectroscopy [8, 9], positive photoion mass spectrometry [10–12], and photoelectron photoion coincidence spectroscopy [13]. The energetic thresholds for the bond-fissions of CFC₃ were accurately determined by a threshold photoelectron photoion coincidence (TPEPICO) study [14]. In the photodissociations, positive ion-negative ion (also known as ion-pair) dissociation is a novel process, firstly proposed by Ajello *et al.* for CFC₃ [12]. Schenk *et al.* found that some ion-pair photodissociations of this molecule could occur at 13.7±0.5 eV and 15.2±0.1 eV (CFC₃→Cl⁺+CCl₂+F⁻) and 15.6±0.1 eV (CFC₃→CFCl+Cl⁺+Cl⁻) [11]. The

energetic threshold of CFC₃→CFCl₂⁺+Cl⁻ was determined to be 7.95±0.20 eV [15]. However, the dynamic and thermochemical information on the ion-pair photodissociations of CFC₃ is still very limited besides above three experimental studies [11, 12, 15]. In this work, we report an experimental study of the ion-pair dissociations of CFC₃ in a broad vacuum UV (VUV) energy range of 7.75–22.00 eV using the synchrotron radiation facility at Hefei, China. Two anionic fragments F⁻ and Cl⁻ are observed in the negative ion mass spectra. The ion-pair anion efficiency spectra (IPAES) of the isotope anions ³⁵Cl⁻ and ³⁷Cl⁻ are recorded.

The procedure to record IPAES is similar to that for positive photoion efficiency spectrum, namely, in the former case the signals of the anion produced in the ion-pair dissociations are collected with scanning the VUV photon energy [16–18]. To access the ion-pair dissociation channel, for example, the energetic threshold $E_{\text{threshold}}$ of the ion-pair dissociation of a diatomic molecule AB: AB+hν→A⁺+B⁻ is determined by,

$$E_{\text{threshold}} = D_0(A^+ - B) + IP_a(AB) - EA(B) \quad (1)$$

where D_0 is the dissociation energy of (AB)⁺ to A⁺ and B, $IP_a(AB)$ is the molecular adiabatic ionization potential, and $EA(B)$ is the electron affinity of B. In the IPAES, the first onset of the efficiency curve for a specific anion corresponds to its appearance energy (AE). AE is usually approximated to be $E_{\text{threshold}}$ of the ion-pair dissociation if the dynamic energy barrier in the dissociation channel is not considered. Any one term can be deduced with the other three terms in Eq.(1), thus the AE values determined in the IPAES

* Author to whom correspondence should be addressed. E-mail: sxtian@ustc.edu.cn

are of utmost importance in thermochemistry. When $EA(B) < D_0(A^+ - B)$, the B^- can be produced at the photon energy higher than the ionization threshold, *i.e.*, $IP_a(AB)$. In this case, the photoelectron may also lead to B^- yields through the dissociative photoelectron attachments (DEAs) to the parent molecule AB . This will interfere with the anionic signals in the IPAES [15]. When $EA(B) > D_0(A^+ - B)$, such interference will be diminished because $E_{\text{threshold}}(B^-)$ is lower than $IP_a(AB)$ and there are no photoelectrons in the reaction area. In this work, the VUV photon energy is extended to be 7.75 eV which is much lower than the IP_a value of $CFCl_3$, thereby the $E_{\text{threshold}}$ values are precisely determined without any interference of the DEAs. In the previous experimental work, the photoionization yield of Cl^- due to that the DEAs was found to be much stronger than that produced in the ion-pair dissociation [15]. As for the photon energy higher than the ionization threshold, much more care should be taken to remove the interference of the DEAs with the anionic yields of the ion-pair dissociations.

II. EXPERIMENTAL METHODS AND THERMOCHEMISTRY CALCULATIONS

The ion-pair photodissociation experiments of $CFCl_3$ were carried out at the atomic and molecular physics end-station of national synchrotron radiation facility at Hefei, China. The apparatus used in the present study was described previously in detail [18–20]. Briefly, the VUV photon beam was monochromatized with the undulator-based spherical-gratings (made by Horiba Jobin Yvon in France), then focused onto the reaction region. A diffuse molecular beam was introduced with a stainless steel tube with diameter of 0.5 mm. The anionic fragments were collected with a home-made reflectron time-of-flight mass spectrometer which was installed perpendicularly to the plane containing the molecular beam and the photon beam. Packets of anions were pushed periodically from the reaction region by a pulsed repeller (-165 V voltage, 1.5 – 2.0 μ s pulse width, and 18 kHz repetition) into an acceleration region. The pulsed anions were focused and transferred through the drift area, then reflected by the retarding lenses. At last the anions were detected with two zigzag stacking microchannel plates. The wavelength of VUV beam was calibrated and the energy resolution was determined ($E/\Delta E = 5 \times 10^3$) before the present experiments. The energy scanning step and the signal accumulation time at each step were typically 0.02 eV and 60 s for the photon energies less than 16.40 eV, while 0.06 eV and 60 s for the higher energies. At the photon energy above the ionization threshold, the sample intensities in the reaction areas were tuned to be low enough, the photoelectron attachments as the secondary reactions can be diminished, thus the interference of the anionic fragments produced in the DEAs can be ruled

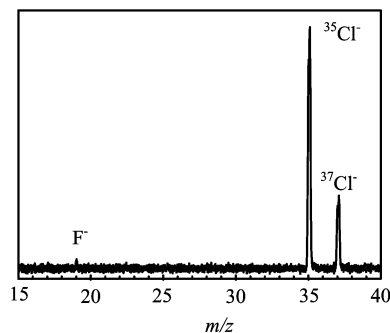


FIG. 1 Anion mass spectrum recorded at the photon energy 18.00 eV.

out. To normalize the anion signals, the photon flux was monitored with a silicon photodiode (SXUV-100, International Radiation Detectors, Inc.). The commercial sample $CFCl_3$ (purity $>99.9\%$) was used after several freeze-pump-thawed cycles.

With Eq.(1), we calculated the enthalpy changes of the possible ion-pair dissociations of $CFCl_3$. The corrections to AE value (at 298 K, since the room-temperature diffuse beam was employed in this work) when it is approximated to be $\Delta_r H_{298}^\ominus$ are typically only 0.05 – 0.15 eV [21], and can be ignored in some extent. The effects of entropy are disregarded, which leads to the more negative $\Delta_r G_{298}^\ominus$ with respect to the calculated $\Delta_r H_{298}^\ominus$ values. The formation enthalpy $\Delta_f H^\ominus$ -288.7 kJ/mol at 298 K of $CFCl_3$ and the enthalpies of the daughter ions and the neutral fragments (at 0 K) at the ground states given in the JANAF tables [22] were used to calculate the ion-pair dissociation energies. Here the internal energies of the daughter ions and fragments were excluded. When the enthalpy values of the fragments at 0 K were unavailable, the data for cations, CCl^+ , $CClF^+$, CCl_2^+ , and $CFCl_2^+$, at 298 K from Lias *et al.* were used [23]. Note that the $\Delta_f H^\ominus$ values of Cl_2^+ and FCl^+ were obtained indirectly [24]. The $\Delta_f H^\ominus$ values of $CFCl$ at the ground and excited ($\tilde{A}^1 A''$) states were cited from Refs.[25, 26]. The $\Delta_f H^\ominus$ values of CCl^+ at $a^3 \Pi_1$ and $A^1 \Pi$ states were cited from Ref.[27]. The threshold of the dissociation $Cl_2^+ + CF(B^2 \Delta) + Cl^-$ was estimated [28] with the thermochemical values obtained by Secombe *et al.* [9]. It is noted again that the calculated $E_{\text{threshold}}$ using above thermochemical data may not be exactly equal to the experimental AE value for a certain anionic fragment, because the possible dynamic energy barrier of the ion-pair dissociation was not considered in Eq.(1).

III. RESULTS AND DISCUSSION

As shown in Fig.1, the anionic fragments F^- and Cl^- (including its two isotopes $^{35}Cl^-$ and $^{37}Cl^-$) were detected at the photon energy 18.00 eV. The signal intensity of F^- is too weak to be detected at the lower ener-

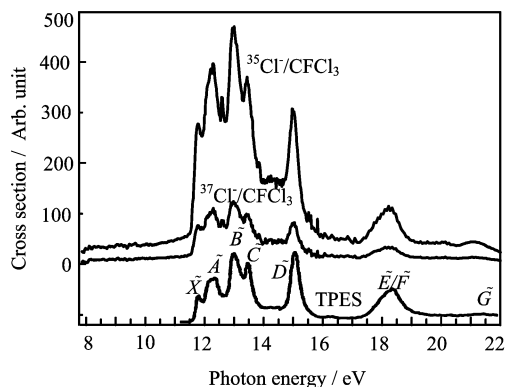


FIG. 2 The anion yield spectra for $^{35}\text{Cl}^-$ and $^{37}\text{Cl}^-$ and the threshold photoelectron spectrum (TPES) of CFCl_3 (reproduced from Ref.[14] with the copyright permission from RSC publishing).

gies. Therefore, only the IPAES of Cl^- were recorded and plotted in Fig.2, together with the threshold photoelectron spectrum (TPES) [14] for comparison. The electron configuration of the ground-state CFCl_3 is

$$\underbrace{(\text{core})^{34} (1a_1)^2 (2a_1)^2 (1e)^4}_{\text{Inner-valence}} \underbrace{(3a_1)^2 (4a_1)^2 (2e)^4 (3e)^4 (5a_1)^2 (4e)^4 (5e)^4 (1a_2)^2}_{\text{Outer-valence}}$$

thus the ionization states shown in the TPES, \tilde{X} , \tilde{A} , \tilde{B} , \tilde{C} , \tilde{D} , \tilde{E} , \tilde{F} , and \tilde{G} , correspond to the electron removing from the outer-valence MOs $1a_2$, $5e$, $4e$, $5a_1$, $3e$, $2e$, $4a_1$, and $3a_1$, respectively. Here the first four MOs are of Cl lone-pair characters, $3e$, $2e$, and $4a_1$ are of CCl_3 bonding/F lone-pair characters, and $3a_1$ is basically of C2s orbital [9]. In the IPAES, the most of the peaks are related to these ionization states, namely, some ion-pair dissociation channels are coupling the series of Rydberg states converging to the respective ionization states,

$$E_R = \text{IP}_v - \frac{R}{(n - \delta)^2} \quad (2)$$

where E_R is the energy of Rydberg state, IP_v is the molecular vertical ionization potential, R is the Rydberg constant (13.60569 eV), n is the principal quantum number, and δ is the quantum defect resulting from the penetration of the Rydberg orbital into the core. When the Rydberg state strongly couples some ion-pair dissociation channel, the anionic fragment signals will be resonantly enhanced. The strong peaks at 11.76, 12.24, 12.95, 13.44, 15.01, and 18.21 eV in the IPAES indicate that the ion-pair dissociation channels remarkably couple the high Rydberg states converging to the ionization states \tilde{X} , \tilde{A} , \tilde{B} , \tilde{C} , \tilde{D} , \tilde{E} , and \tilde{F} , respectively. The IPAES both of $^{35}\text{Cl}^-$ and $^{37}\text{Cl}^-$ show the same features, implying that the isotopic effect on the ion-pair dissociations is rather weak. Therefore, in the following text, we

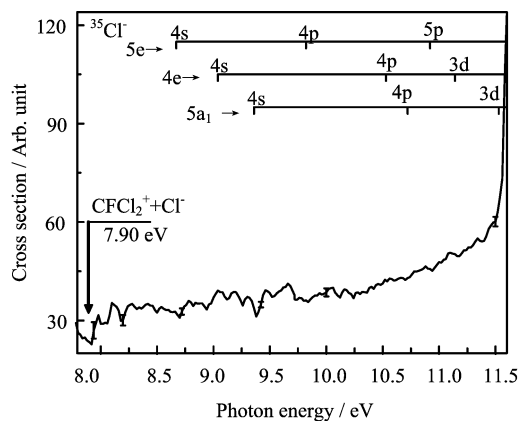


FIG. 3 The anion yield spectrum of Cl^- in the lower photon energy range. The experimental uncertainties are labeled with error bars at the selected energy points. The electron valence-to-Rydberg transitions and the threshold of $\text{CFCl}_3 \rightarrow \text{CFCl}_2^+ + \text{Cl}^-$ are tentatively assigned.

TABLE I Rydberg assignments to the Cl^- efficiency curve in the energy range of 7.75–11.60 eV.

Energy/eV [8]	Assignment	δ
8.67	4s←5e	2.02
9.04	4s←4e	2.14
9.36	4s←5a ₁	2.17
9.82	4p←5e	1.56
10.16	3d←5e	0.37
10.53	4p←4e	1.63
10.72	4p←5a ₁	1.76
10.92	5p←5e	1.64
11.14	3d←4e	0.27
11.53	3d←5a ₁	0.31
11.53	4s←3e	2.02

only focus on the production efficiency curve of $^{35}\text{Cl}^-$. Furthermore, in contrast to the TPES, some additional peaks or spectral characters are observed in the IPAES, namely, a small but distinct peak at 12.60 eV, a basin existing in the energy range of 13.90–14.77 eV, and a band shoulder extending from 15.42 eV to 16.00 eV. At the lower photon energy range, an onset of the production efficiency curve is observed at 7.94 eV.

In Fig.3, one can zoom in the Cl^- efficiency curve in the energy range of 7.75–11.60 eV for details. In this energy range, the electron transitions from the valence to Rydberg orbitals have been observed in the photoabsorption spectra [2, 6–8]. The assignments by Ibuki *et al.* [8] are adopted in the present work, see Fig.3 and Table I. Although the signal strengths of Cl^- are beyond the experimental uncertainties (error bars are exhibited for the selected energy points in Fig.3), there are no strong peaks in the efficiency curve. This implies that the coupling between the ion-pair dissociations and

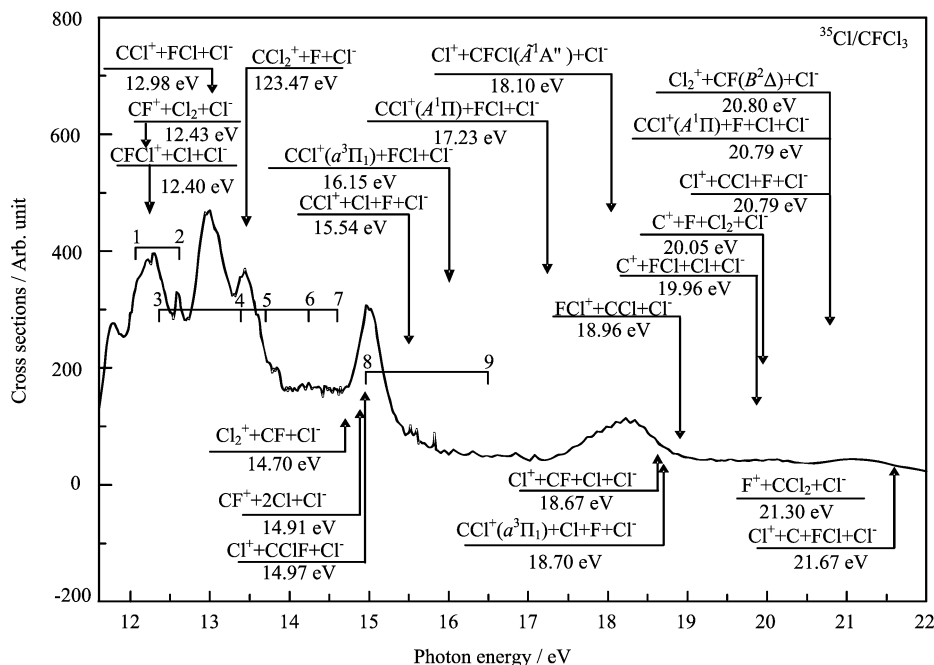


FIG. 4 The electron valence-to-Rydberg transitions (1–9) and the multibody fragmentation channels are tentatively assigned in the anion yield spectrum of Cl^- .

the electron valence-to-Rydberg transitions (assigned in Fig.3) is quite weak. On the other hand, the onset of the efficiency curve is found at 7.94 ± 0.04 eV which is in excellent agreement with the previous experimental datum 7.95 ± 0.20 eV [15]. The thermochemical threshold of $\text{CFCl}_3 \rightarrow \text{CFCl}_2^+ + \text{Cl}^-$ is estimated to be 7.90 eV in this work, which is slightly different from 7.94 eV given by Ajello and Rayermann [15].

In Tables II and III, the energies of the electron valence-to-Rydberg transitions and the thresholds of the multibody ion-pair fragmentation processes are listed. The electron valence-to-Rydberg transitions are cited from Refs.[6, 7, 10], and used in the present spectral assignments, 1–9, see Fig.4. It is worth noting that the electron transition 2 ($5a_1 \rightarrow 5p$) at ca.12.6 eV happens to correspond to the peak of 12.60 eV in the Cl^- efficiency curve, showing an evidence of the significant coupling between this electron transition and the ion-pair dissociation. The other transitions, 5 ($3e \rightarrow 5p$), 6 ($3e \rightarrow 4d$), and 7 ($3e \rightarrow nl$), may be responsible for the band shoulder around 13.63 eV and the basin in the energy range of 13.90–14.77 eV.

Twenty-one multibody fragmentation channels are assigned in Fig.4, although we cannot exhaust all possible ion-pair dissociation channels in this energy range. Among of them, six channels include the excited-state fragments and are lying at the relatively high energies. $\text{CF}(B^2\Delta)$ daughter fragment has been detected with the VUV fluorescence spectroscopy, indicating that it is produced in the energy range of 16.0–20.7 eV [9]. As mentioned above, the strong peaks at 12.24, 12.95, 13.44, and 15.01 eV in the IPAES are related to the

TABLE II Rydberg assignments to the Cl^- efficiency curve in the energy range of 11.60–22.00 eV.

Peak number	Energy/eV			Assignment
	Ref.[7]	Ref.[10]	Ref.[6]	
1	12.07	12.05		$5s \leftarrow 5a_1, 5p \leftarrow 4e$
2	12.62	12.60	12.59	$5p \leftarrow 5a_1$
3	12.36			$4p \leftarrow 3e$
4	12.39			$3d \leftarrow 3e$
5	13.70	13.60	13.76	$5p \leftarrow 3e$
6	14.24			$4d \leftarrow 3e$
7	14.60			$nl \leftarrow 3e$
8	14.95	15.00	14.91	$3s \leftarrow 4a_1/2a_1$
9	16.48	16.70	16.52	$4s, 3p, 3d \leftarrow 4a_1/2a_1$

electron valence-to-Rydberg transitions converging to \bar{A} , \bar{B} , \bar{C} , \bar{D} , and \bar{E} ionization states, respectively. In Fig.4, some specific ion-pair dissociation channels $\text{CFCl}_3 \rightarrow \text{CFCl}^+ + \text{Cl} + \text{Cl}^-$ (12.40 eV), $\text{CFCl}_3 \rightarrow \text{CF}^+ + \text{Cl}_2 + \text{Cl}^-$ (12.49 eV), $\text{CFCl}_3 \rightarrow \text{CCl}^+ + \text{FCl} + \text{Cl}^-$ (12.98 eV), $\text{CFCl}_3 \rightarrow \text{CCl}_2^+ + \text{F} + \text{Cl}^-$ (13.47 eV), $\text{CFCl}_3 \rightarrow \text{CF} + \text{Cl}_2^+ + \text{Cl}^-$ (14.70 eV), $\text{CFCl}_3 \rightarrow \text{CF}^+ + 2\text{Cl} + \text{Cl}^-$ (14.91 eV), $\text{CFCl}_3 \rightarrow \text{CFCl} + \text{Cl}^+ + \text{Cl}^-$ (14.97 eV), may couple the electron valence-to-Rydberg transitions converging to the ionization states, *i.e.*, \bar{A} , \bar{B} , \bar{C} , \bar{D} , and \bar{E} , because the thresholds of these ion-pair dissociations are very close to their respective IP_v values.

According to the thermochemical values, two thresh-

TABLE III Energetics of the multibody ion-pair dissociations to produce Cl^- and vertical ionization potentials of CFCl_3 .

Neutral	Ion-pair dissociation	$E_{\text{threshold}}/\text{eV}$	IP_v/eV		
			Ref.[5]	Ref.[9]	Ref.[4]
$\text{CFCl}_3^+(\tilde{G}^2\text{A}_1)$	$\text{Cl}^+ + \text{C} + \text{FCl} + \text{Cl}^-$	21.67	21.50	21.44	
	$\text{F}^+ + \text{CCl}_2 + \text{Cl}^-$	21.30			
	$\text{Cl}_2^+ + \text{CF}(B^2\Delta) + \text{Cl}^-$	20.80			
	$\text{CCl}^+(A^1\Pi) + \text{F} + \text{Cl} + \text{Cl}^-$	20.79			
	$\text{Cl}^+ + \text{CCl} + \text{F} + \text{Cl}^-$	20.79			
	$\text{C}^+ + \text{F} + \text{Cl}_2 + \text{Cl}^-$	20.05			
	$\text{C}^+ + \text{FCl} + \text{Cl} + \text{Cl}^-$	19.96			
	$\text{FCl}^+ + \text{CCl} + \text{Cl}^-$	18.96			
	$\text{CCl}^+(a^3\Pi_1) + \text{Cl} + \text{F} + \text{Cl}^-$	18.70			
$\text{Cl}^+ + \text{CF} + \text{Cl} + \text{Cl}^-$	18.67				
$\text{CFCl}_3^+(\tilde{F}^2\text{A}_1)$	$\text{Cl}^+ + \text{CFCl}(\tilde{A}^1\text{A}'') + \text{Cl}^-$	18.10	18.40	18.33	
$\text{CFCl}_3^+(\tilde{E}^2\text{E})$	$\text{CCl}^+(A^1\Pi) + \text{FCl} + \text{Cl}^-$	17.23	18.00	18.33	
	$\text{CCl}^+(a^3\Pi_1) + \text{FCl} + \text{Cl}^-$	16.15			
	$\text{CCl}^+ + \text{Cl} + \text{F} + \text{Cl}^-$	15.54			
$\text{CFCl}_3^+(\tilde{D}^2\text{E})$	$\text{Cl}^+ + \text{CClF} + \text{Cl}^-$	14.97	15.05	15.04	15.008
	$\text{CF}^+ + 2\text{Cl} + \text{Cl}^-$	14.91			
	$\text{Cl}_2^+ + \text{CF} + \text{Cl}^-$	14.70			
	$\text{CCl}_2^+ + \text{F} + \text{Cl}^-$	13.47			
	$\text{Cl}^+ + \text{CClF} + \text{Cl}^-$	14.97			
$\text{CFCl}_3^+(\tilde{C}^2\text{A}_1)$	$\text{CCl}^+ + \text{FCl} + \text{Cl}^-$	12.98	13.45	13.45	13.462
$\text{CFCl}_3^+(\tilde{B}^2\text{E})$	$\text{CF}^+ + \text{Cl}_2 + \text{Cl}^-$	12.43	12.97	12.99	13.10
	$\text{CFCl}^+ + \text{Cl} + \text{Cl}^-$	12.40			
	$\text{CF}^+ + \text{Cl}_2 + \text{Cl}^-$	12.43			
$\text{CFCl}_3^+(\tilde{A}^2\text{E})$			12.13	12.31	12.32
$\text{CFCl}_3^+(\tilde{X}^2\text{A}_2)$			11.73	11.78	11.76
	$\text{CFCl}_2^+ + \text{Cl}^-$	7.90			
$\text{CFCl}_3(\tilde{X}^1\text{A}_1)$			0.00		

olds of the ion-pair dissociation channels to produce $\text{CCl}^+(a^3\Pi_1)$ are 16.15 and 18.70 eV. It is usually forbidden to produce the triplet state $\text{CCl}^+(a^3\Pi_1)$ in the single photon absorption, but the ion-pair dissociation channels can be accessed by the system-transitions through a conical cone between the singlet and triplet potential energy surfaces. Unfortunately, the high-lying excited-state potential energy surfaces of this molecule are still unexplored. The present tentative assignments may be guidance to the further studies. Furthermore, the differences between the present dissociation thresholds (in Table III) and the experimental AEs reported previously [10–12, 14] should be addressed. The AE values for CCl_2F^+ produced in the photoexcitations of CFCl_3 were 11.65 [10], 11.57 [12], and 11.53 ± 0.05 eV [14]. In this work, the lowest threshold to produce CCl_2F^+ is 7.90 eV (thermochemical value)

or 7.94 ± 0.04 eV ($\text{CFCl}_3 \rightarrow \text{CFCl}_2^+ + \text{Cl}^-$). Such distinct difference should be due to the low sensitivity of the previous mass spectrometers [10, 12] and the completely different technique (TPEPICO) used by Secombe *et al.* [14]. In the TPEPICO experiment [14], only the daughter cations produced in the dissociative photoionization can be studied. In the similar scenario, such significant differences are also found for CCl^+ , CF^+ , CFCl^+ , and CCl_2^+ . Therefore, in contrast to the dissociative photoionizations, the daughter ions may be produced at the much lower photon energy through the ion-pair dissociations. The threshold of a multibody fragmentation $\text{CFCl}_3 \rightarrow \text{CFCl} + \text{Cl}^+ + \text{Cl}^-$ was determined to be 15.6 ± 0.1 eV [11]. However, its threshold is predicted with Eq.(1) to be 14.97 eV. As mentioned above, the experimental AE for a certain ion represents the activation energy of the dissociation channel. Thus the

energy barrier of this dissociation channel may be deduced to be 0.6 eV. For another multibody fragmentation $\text{CFCl}_3 \rightarrow \text{CFCl}^+ + \text{Cl} + \text{Cl}^-$, its threshold was proposed to be 16.02 eV [12] which is much higher than the present thermochemical value 12.40 eV. Such unusual high energy barrier with more than 3.6 eV may be unacceptable. The reliable AE for the multibody ion-pair fragmentation can be accurately determined with the positive-negative photoions coincidence spectroscopy.

IV. CONCLUSION

Ion-pair photodissociations of CFCl_3 are investigated with the negative ion mass spectrometry based on synchrotron radiation facility. Anionic fragments, F^- and Cl^- (two isotope species $^{35}\text{Cl}^-$ and $^{37}\text{Cl}^-$), are observed. The ion-pair anion efficiency spectra of $^{35}\text{Cl}^-$ and $^{37}\text{Cl}^-$ are recorded in the photon energy range of 7.75–22.00 eV. The threshold of ion-pair dissociation $\text{CFCl}_3 \rightarrow \text{CFCl}_2^+ + \text{Cl}^-$ is experimentally determined to be 7.94 ± 0.04 eV, in excellent agreement with the values reported in the Ref.[15]. With the references of the high-resolution photoabsorption spectra [2, 6–8], the electron transitions from the valence to Rydberg orbitals are assigned in the Cl^- efficiency spectrum. The multibody ion-pair fragmentation processes to produce Cl^- are discussed by comparison between the calculated thermochemical thresholds and the experimental efficiency spectrum.

V. ACKNOWLEDGMENTS

This work is supported by the National Natural Science Foundation of China (No.10775130 and No.10979048), the Ministry of Science and Technology (No.2007CB815204 and No.2011CB921401), the USTC-NSRL association funding, and the Fundamental Research Funds for the Central Universities (No.WK2340000012).

- [1] M. J. Molina and F. S. Rowland, *Rev. Geophys. Space* **13**, 1 (1975).
- [2] J. Doucet, P. Sauvageau, and C. Sandorfy, *J. Chem. Phys.* **58**, 3708 (1973).
- [3] F. T. Chau and C. A. McDowell, *J. Electron Spectrosc. Relat. Phenom.* **6**, 357 (1975).
- [4] R. Jadry, L. Karlsson, L. Mattsson, and Siegbahn, *Phys. Script.* **16**, 235 (1977).

- [5] T. Cvitaš, H. Güten, and L. Klasinc, *J. Chem. Phys.* **67**, 2687 (1977).
- [6] R. Gilbert, P. Sauvageau, and C. Sandorfy, *J. Chem. Phys.* **60**, 4820 (1974).
- [7] G. C. King and J. W. McConkey, *J. Phys. B* **11**, 1861 (1978).
- [8] T. Ibuki, A. Hiraya, and K. Shobatake, *J. Chem. Phys.* **90**, 6290 (1989).
- [9] D. P. Seecombe, R. R. Tuckett, H. Baumgärtel, and H. W. Jochims, *Phys. Chem. Chem. Phys.* **1**, 773 (1999).
- [10] H. W. Jochims, W. Lohr, and H. Baumgärtel, *Ber. Bunsen-Ges. Phys. Chem.* **80**, 130 (1976).
- [11] H. Schenk, H. Oertel, and H. Baumgärtel, *Ber. Bunsen-Ges. Phys. Chem.* **83**, 683 (1979).
- [12] J. M. Ajello, W. T. Huntress Jr., and P. Rayermann, *J. Chem. Phys.* **64**, 4746 (1976).
- [13] W. Kischlat and H. Morgner, *J. Electron Spectrosc. Relat. Phenom.* **35**, 273 (1984).
- [14] D. P. Seecombe, R. Y. L. Chim, G. K. Jarvis, and R. R. Tuckett, *Phys. Chem. Chem. Phys.* **2**, 769 (2000).
- [15] J. M. Ajello and P. Rayermann, *J. Chem. Phys.* **71**, 1512 (1979).
- [16] S. Suzuki, K. Mistuke, T. Imamura, and I. Koyano, *J. Chem. Phys.* **96**, 7500 (1992).
- [17] M. J. Simpson and R. P. Tuckett, *J. Phys. Chem. A* **114**, 8043 (2010).
- [18] S. X. Tian, Y. F. Xu, Y. F. Wang, Q. Feng, L. L. Chen, J. D. Sun, F. Y. Liu, X. B. Shan, and L. S. Sheng, *Chem. Phys. Lett.* **496**, 254 (2010).
- [19] Q. Feng, S. X. Tian, Y. J. Zhao, F. Y. Liu, X. B. Shan, and L. S. Sheng, *Chin. Phys. Lett.* **26**, 053402 (2009).
- [20] L. L. Chen, Y. F. Xu, Q. Feng, S. X. Tian, F. Y. Liu, X. B. Shan, and L. S. Sheng, *J. Phys. Chem. A* **115**, 4248 (2011).
- [21] J. C. Traeger and R. G. McLoughlin, *J. Am. Chem. Soc.* **103**, 3647 (1981).
- [22] M. W. Chase, *J. Phys. Chem. Ref. Data Monogr.* **9**, (1998).
- [23] S. G. Lias, J. E. Bartmess, J. F. Liebman, J. L. Holmes, R. D. Lerin and W. G. Mallard, *J. Phys. Chem. Ref. Data Suppl.* **17**, 1 (1988).
- [24] (a) R. L. DeKock, B. R. Higginson, D. R. Lloyd, A. Breeze, D. W. J. Cruickshank, and D. R. Armstrong, *Mol. Phys.* **24**, 1059 (1972)
(b) J. Li, Y. S. Hao, J. Yang, C. Zhou, and Y. X. Mo, *J. Chem. Phys.* **127**, 104307 (2007).
- [25] C. F. Rodriguez and A. C. Hopkinson, *J. Phys. Chem.* **97**, 849 (1993).
- [26] M. E. Jacox, *J. Phys. Chem. Ref. Data Monogr.* **3**, (1994).
- [27] M. Tsuji, T. Mizuguchi, K. Shinohara, and Y. Nishimura, *Can. J. Phys.* **61**, 838 (1983).
- [28] J. D. D. Martin and J. W. Hepburn, *J. Chem. Phys.* **109**, 8139 (1998).